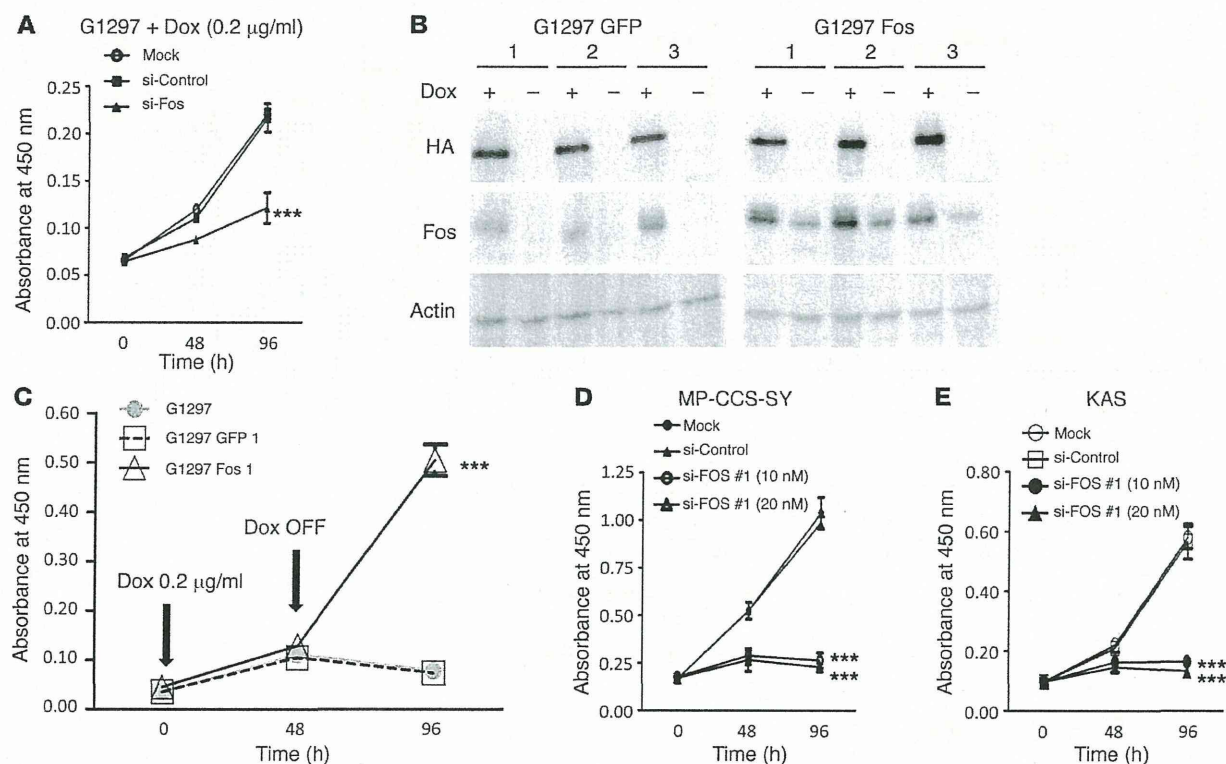


research article

**Figure 6**

Fos plays a key role in *EWS/ATF1*-induced cell proliferation. (A) Effect of *Fos* knockdown on proliferation of *EWS/ATF1*-induced cells. G1297 cells were treated with siRNA targeting *Fos* (si-Fos; 10 nM), a control siRNA (si-Control; 10 nM), or lipofectamine alone (Mock). 48 and 96 hours later, cell viability was determined by WST-8 assay. Results are mean \pm SD ($n = 4$). *** $P < 0.001$ vs. si-Control and Mock. (B) *EWS/ATF1*-induced tumor cell lines overexpressing *Fos* or *EGFP* (G1297 Fos and G1297 GFP, respectively). pCAG-*Fos*-IZ vector or pCAG-*EGFP*-IZ vector were stably transfected in G1297 cells. Western blot analysis revealed that G1297 Fos cells stably expressed Fos protein even in the absence of doxycycline. (C) Cell proliferation assay for G1297, G1297 GFP, and G1297 Fos cells before and after doxycycline withdrawal. Doxycycline treatment (0.2 µg/ml) was withdrawn for 48 hours. Cell viability was determined by WST-8 assay. *** $P < 0.001$ vs. G1297 GFP. (D and E) Effect of *FOS* knockdown on growth of human CCS cell lines. MP-CCS-SY and KAS cells were treated with siRNA#1 targeting *FOS* (si-FOS #1; 10 nM and 20 nM), control siRNA (si-Control; 20 nM), or lipofectamine alone (Mock). 48 and 96 hours later, cell viability was determined by WST-8 assay. Data are mean \pm SD ($n = 4$). *** $P < 0.001$ vs. si-Control and Mock.

(Supplemental Figure 7D), phosphorylation of ERK1/2 was not observed in the *EWS/ATF1*-induced tumor cell line, even after serum stimulation (Supplemental Figure 7E), which suggests that continuous upregulation of *Fos* in *EWS/ATF1*-induced tumor cells is independent of the RAS/Raf/ERK signaling pathway. We treated *EWS/ATF1*-induced tumor cells with the MEK inhibitor U0126 to block activation of ERK1/2 in order to further confirm the ERK-independent activation of *Fos*. Although inhibition of ERK1/2 resulted in a substantial decrease of *Fos* in MEFs, U0126 failed to suppress *Fos* expression in *EWS/ATF1*-induced tumor cells (Figure 5C). These data indicate that constitutive overexpression of *Fos* in *EWS/ATF1*-induced tumor cells was mediated by an ERK-independent mechanism.

Previous studies demonstrated an interaction of ATF1 at a CRE in the *Fos* promoter (34, 35), which suggests that *EWS/ATF1* may induce *Fos* expression through interaction with the CRE. Conversely, in the present study, regulatory motif analysis of the upregulated genes by *EWS/ATF1* demonstrated enrichment of CRE near the transcription start site (from -1,000 bp to +200 bp; Supplemental Figure 6B). To evaluate the functional importance of this element in *EWS/ATF1*-mediated activation of *Fos*, we constructed a reporter plasmid con-

taining the mouse *Fos* promoter with wild-type and mutated CRE and examined transcriptional activity by luciferase assay (Figure 5D). We confirmed that induction of *EWS/ATF1* resulted in remarkably increased *Fos* promoter activity with wild-type CRE in G1297 cells. Importantly, luciferase activity of the mutated promoter significantly decreased compared with that of the wild-type promoter. We further examined whether *EWS/ATF1* directly binds to the CRE of the *Fos* promoter. ChIP-PCR analysis revealed that doxycycline-induced *EWS/ATF1* was enriched at the CRE of the *Fos* promoter, but not at the negative control cis element (Figure 5E). Our results indicated that the CRE is crucial for *EWS/ATF1*-mediated transcriptional activity of *Fos* in *EWS/ATF1*-induced tumor cells.

Expression of *FOS* in human CCS. To investigate whether overexpression of *FOS* is linked to human CCS, we analyzed *FOS* expression in the human CCS cell lines MP-CCS-SY and KAS and in the control lung fibroblast cell line WI38 by qRT-PCR. *FOS* was found to be highly expressed in both human CCS cell lines compared with WI38 (Supplemental Figure 8A). We also found that surgically resected clinical CCS specimens also expressed higher levels of *FOS* than did WI38 (Supplemental Figure 8B), which indicates that human CCS expresses higher levels of *FOS*.



We examined the effect of *EWS/ATF1* knockdown on *FOS* expression in human CCS cell lines to further investigate the association between *EWS/ATF1* expression and increased *FOS* expression in human CCS. Human CCS cell lines MP-CCS-SY and KAS carry the *EWS/ATF1* type 1 and type 2 fusion genes, respectively (Supplemental Figure 9, A and B). We next designed a specific siRNA targeting the breakpoint of the *EWS/ATF1* type 1 fusion gene, which had no effect on the expression of *ATF1* or of the *EWS/ATF1* type 2 fusion gene in KAS (Supplemental Figure 9, E and F). siRNA treatment targeting *EWS/ATF1* type 1 in MP-CCS-SY led to significant downregulation of *FOS* 48 hours after treatment (Supplemental Figure 9G) as well as of *EWS/ATF1* type 1 itself (Supplemental Figure 9, C and D), which indicates that *FOS* is a direct target of *EWS/ATF1* in human CCS. In contrast to *FOS*, we observed a modest reduction of *MITF-M* expression after *EWS/ATF1* knockdown in MP-CCS-SY cells (Supplemental Figure 9H).

FOS could be a promising therapeutic target for human CCS. To examine whether *Fos* overexpression facilitates proliferation of tumor cells expressing *EWS/ATF1*, we knocked down *Fos* in *EWS/ATF1*-induced tumor cells using siRNA. The G1297 cell line was treated with siRNA for *Fos* in the presence of doxycycline. siRNA treatment (10 nM) decreased the expression of *Fos* at the mRNA level by 75% at 24 hours after transfection, although it had no effect on expression of the *EWS/ATF1* transgene compared with the control siRNA (Supplemental Figure 10A). In addition, we confirmed that *Fos* protein levels were also decreased 48 hours after transfection (Supplemental Figure 10B). A WST-8 assay was performed in *EWS/ATF1*-induced tumor cells transfected with the nonfunctional control siRNA or with functional *Fos* siRNA to examine the effect of *Fos* knockdown on the cellular kinetics. The siRNA targeting *Fos* efficiently inhibited cell proliferation of *EWS/ATF1*-induced tumor cells, even in the presence of doxycycline (Figure 6A). In order to further confirm the importance of *Fos* expression for *EWS/ATF1*-induced tumor cell growth, we established *EWS/ATF1*-induced tumor cell lines in which *Fos* is overexpressed (Figure 6B). We found that *Fos*-overexpressed *EWS/ATF1*-inducible cells retained the ability to proliferate for at least 48 hours after doxycycline withdrawal, whereas control cells in which *GFP* is overexpressed stopped their proliferation soon after withdrawal (Figure 6C). We also examined the effect of *FOS* knockdown on cell growth of human CCS cell lines using siRNA targeting *FOS*. Consistent with the results in *EWS/ATF1*-induced tumor cells, siRNA treatment strongly suppressed the growth of CCS cell lines (Figure 6, D and E, and Supplemental Figure 11, A–F). Taken together, these data suggest that *FOS*, a direct target of *EWS/ATF1*, mediates the oncogenic growth of *EWS/ATF1*-related sarcomas and could be a potent therapeutic target for human CCS.

Discussion

The current study revealed that forced expression of the *EWS/ATF1* fusion gene induced sarcoma formation in *EWS/ATF1* transgenic mice. The histology of the tumors in *EWS/ATF1* transgenic mice showed a striking similarity to that of human CCS. In addition, immunohistochemistry demonstrated that *EWS/ATF1*-induced tumor cells express neural crest-associated markers, such as *S100*, *Mitf*, and *Sox10*, which are also expressed in human CCS. Given that the *EWS/ATF1* fusion gene is detected in CCS, our *EWS/ATF1* transgenic mouse is the first mouse model for investigating CCS pathogenesis. Our present results demonstrated that continuous expression of *EWS/ATF1* was required for growth and tumor

formation of *EWS/ATF1*-induced tumor cells. These results indicate that *EWS/ATF1* plays a pivotal role in both development and maintenance of *EWS/ATF1*-associated sarcomas, implying that CCS exhibits oncogene addiction (36) to *EWS/ATF1*, and provide a rationale for targeting *EWS/ATF1* itself to treat CCS.

It is interesting to note that sarcoma formation was observed only in deep soft tissue, although *EWS/ATF1* was induced in a variety of cell types in this experimental system (37, 38). In addition, the cell proliferation rate of MEFs in vitro was reduced by *EWS/ATF1* induction. These results clearly demonstrated that the abnormal proliferation by the forced expression of *EWS/ATF1* requires a specific cell type of origin, accompanied by a specific microenvironment. Consistent with these findings, recent studies of other sarcoma-related genes revealed that introduction of *SYT/SSX*, a synovial sarcoma-related gene, into *Myf5*-positive immature myoblasts specifically resulted in sarcoma formation, whereas its expression in more differentiated cells induced myopathy without tumor induction (39). In addition, introduction of *EWS/FLI1*, a fusion gene detectable in Ewing sarcomas, results in transformation specifically in bone marrow-derived mesenchymal progenitor cells in vitro (40). Taken together, these findings are suggestive of cell type-specific carcinogenesis by expression of sarcoma-related fusion oncogenes.

Our lineage-tracing experiments in vivo suggested that *EWS/ATF1*-associated tumor cells are derived from neural crest-derived cells. This result is consistent with several lines of evidence that CCS often shows melanocytic differentiation and resembles MM. However, our present results do not exclude the possibility that *EWS/ATF1*-induced tumors can arise from non-neural crest-derived cells. In addition, the exact cell type of origin of *EWS/ATF1*-induced tumors remains unclear, since neural crest-lineage progenitors can differentiate into many different cell types, such as neuronal cells, melanocytes, and Schwann cells. Recently, Schwann cell precursors along the peripheral nerve have been shown to be a cellular source of large numbers of melanocytes in the skin during development in mice and chicks (41). Moreover, Schwann cells also retain the potential to differentiate into melanocytes, resulting from a loss of nerve contact (41). Given the finding that *EWS/ATF1*-induced tumor cells expressed markers for melanocytic differentiation, it is possible that the neural crest-derived Schwann cells could be the origin of *EWS/ATF1*-associated sarcomas.

We found that *Fos* was one of the direct targets of *EWS/ATF1* in *EWS/ATF1*-induced tumor cells. *Fos* is an immediate early gene that can be activated by a variety of mitogens and growth factors. The present study showed that *Fos* induction by forced expression of *EWS/ATF1* was independent of the ERK signaling pathway. In contrast, we found that *Fos* upregulation was mediated by a CRE of the *Fos* promoter, accompanied by direct interaction of *EWS/ATF1* with the CRE on the *Fos* promoter. The direct interaction of *EWS/ATF1* at CRE may induce continuous transcriptional activation of *Fos* in *EWS/ATF1*-induced tumor cells. Previous studies have demonstrated a higher expression level of *FOS* to be involved in tumor growth in several cancers (42–44), and overexpression of *Fos* results in osteosarcoma formation in transgenic mice (45, 46). Here we showed that *FOS* was also upregulated in CCS by the *EWS/ATF1* fusion transcript and that the increased *FOS* promoted the growth of *EWS/ATF1*-related sarcomas. Accordingly, blocking the *FOS* pathway might be a promising therapeutic strategy for treating CCS (Supplemental Figure 12).

research article

Methods

Molecular cloning and gene targeting in ES cells. Human *EWS/ATF1*-FLAG-HA was amplified by RT-PCR from the human CCS cell line KAS using primers ACATGGCGTCCACGGATTACAG and CCTAGGCGTAGTC-GGGCAGCTCGTAGGGGTATCCTCCAGCGGCCGACTTGTTCATC-GTCGTCCTGTAGTCTCCTCAACACTTTTATTGGAATAAAGAT and cloned into pcr2.1-TOPO. Sequence-verified *EWS/ATF1*-FLAG-HA cDNA was subcloned into a unique *EcoRI* site of pBS31 prime (37, 38). KH2 ES cells (obtained from Open Biosystems) were used to insert a single copy of *EWS/ATF1*-FLAG-HA by Flipase (PLP) recombination into the *Col1A1* locus under the control of a minimal CMV tetracycline-inducible promoter using a previously described method (37), and ES cells were selected for hygromycin resistance.

Mouse generation. For blastocyst injections, fertilized zygotes were isolated from the oviducts of day-0.5 pregnant B6D2F1 females and allowed to develop to the blastocyst stage in culture. 7–12 ES cells were injected per blastocyst. The injected blastocysts were transferred into day-2.5 pseudo-pregnant recipient females.

Doxycycline treatment. 6-week-old mice were administered 50 µg/ml doxycycline (Sigma-Aldrich) in their drinking water supplemented with 2 mg/ml sucrose. For cultured cells, doxycycline was used at a concentration of 0.05–0.2 µg/ml.

RNA preparation and RT-PCR. Total RNA was isolated using a RNeasy mini kit (Qiagen). Total RNA was reverse transcribed using a High-Capacity cDNA Reverse Transcription Kit with RNase inhibitor (Applied Biosystems). qRT-PCR analysis using the fluorescent SYBR green method (Bio-Rad) was performed in accordance with the manufacturer's instructions. The data generated from each reaction were subjected to gene expression analysis using an iCycler iQ Real-Time PCR Detection System (Bio-Rad). See Supplemental Table 1 for specific primer pairs used for amplification. Microarray analysis was performed with SurePrint G3 Mouse GE 8X60K microarray (Agilent Technologies) and Mouse Gene 1.0 ST Array (Affymetrix) according to the manufacturer's instructions. All analyses were performed by Genespring GX (version 12; Agilent Technologies).

Western blot analysis. Western blot analyses were carried out as described previously (47, 48). The following antibodies were used: anti-HA (rabbit IgG, 1:1,000 dilution; Cell Signaling), anti-Fos (rabbit IgG, 1:1,000 dilution; Cell Signaling), anti-ERK1/2 (rabbit IgG, 1:1,000 dilution; Cell Signaling), anti-phospho-ERK1/2 (rabbit IgG, 1:1,000 dilution; Cell Signaling), anti-ATF1 (rabbit IgG, 1:5,000 dilution; EPITOMICS), and anti-β-actin (mouse IgG, 1:5,000 dilution; Calbiochem).

Cell proliferation assay. Cell growth was determined by WST-8 assay using a Cell Counting Kit-8 (Dojindo Laboratories). Absorbance at 450 nm is indicative of the die amount of formazan, which is directly proportional to the number of living cells.

Histological analysis. Normal and tumor tissue samples were fixed in 10% buffered formalin for 24 hours and embedded in paraffin. 4-µm sections were stained with H&E, and serial sections were used for immunohistochemical analyses. Immunostaining was performed using an avidin-biotin immunoperoxidase assay. The primary antibodies used were anti-HA-Tag (1:600 dilution; Cell Signaling), anti-Ki67 (1:250 dilution; Dako), anti-S100 (1:800 dilution; Dako), anti-SOX10 (1:200 dilution; R&D Systems), anti-MITF (1:500 dilution; Exalpath), and anti-GFP (1:1,000 dilution; Abcam).

X-gal staining. Briefly, tumor tissue samples were embedded in OCT compound and frozen. 8-µm cryostat sections were immediately fixed in 0.2% glutaraldehyde for 10 minutes. The sections were stained overnight in an X-gal staining solution, then counterstained with fast red for 3 minutes.

Tumorigenicity studies. 4-week-old male BALB/c athymic mice were obtained from Japan SLC. A total of 5.0×10^6 G1297 cells in 0.1 ml serum-free DMEM was inoculated subcutaneously through a 26-gauge needle

into the posterior flank of each mouse. 3 weeks after inoculation, the tumor diameters were measured with digital calipers, and tumor volume was calculated as $(w^2 \times l)/2$ and expressed in mm³.

siRNA transfection. We performed transient knockdown assays with a siRNA targeting *Fos* (Santa Cruz), *FOS* (Santa Cruz and Dharmacon) or the breakpoint of *EWS/ATF1* type 1 (sense, GCGUGGAAUGGGAAAAAATT; antisense, AUUUUCCCAUCCACCGCTT; KOKEN) using Lipofectamine RNAiMAX (Invitrogen). We used nontargeting siRNA (Cosmo Bio Co.) as a control.

Cell lines. MP-CCS-SY and KAS are CCS cell lines carrying *EWS/ATF1* type 1 and type 2, respectively. MP-CCS-SY was established as described previously (49), and KAS was provided by T. Nakamura (Cancer Institute, Japanese Foundation for Cancer Research, Tokyo, Japan; ref. 24). HOS (osteosarcoma), U2OS (osteosarcoma), NIH3T3 (embryonic fibroblast), and WI38 (lung fibroblast) cells were purchased from the American Type Culture Collection. B16-F1 (mouse melanoma) and A375 (human MM) were purchased from the European Collection of Cell Cultures.

Mice. *Wnt1-Cre* mice were provided by S. Iseki (Tokyo Medical and Dental University, Tokyo, Japan; ref. 50), *P0-Cre* mice were provided by K. Yamamura (Kumamoto University, Kumamoto, Japan; ref. 51), and floxed *LacZ* mice were provided by M. Okabe (Osaka University, Suita, Japan; ref. 52). Floxed *EYFP* mice (53) were obtained from Jackson Laboratory.

Construction of the reporter plasmid. To obtain the *Fos* reporter plasmid (pGL3A-1486), the genomic DNA fragment containing –450 to +0 of the 5'-flanking sequence was amplified by PCR with the primer set 5'-TCTATC-GATAGGTACGAATGTTTCGCTCGCCTTCTC-3' and 5'-ACGCGTA-AGAGCTCGGGAGTAGTAGGGCCCTCAGC-3' and subcloned into the *KpnI* site of the pGL3 vector (Promega). The *Fos* reporter plasmid with mutant CRE element was generated by PCR-targeted mutagenesis with the primer set 5'-CCAGTTCGCCCCACTCAGCTAGGAAGTCCATCC-3' and 5'-GGATGGACTTCTAGCTGAGTGGGCGGAAGTGG-3'.

Luciferase assay. Reporter genes were transfected into the G1297 *EWS/ATF1*-induced tumor cell line together with phRL-SV40 (Promega) using lipofectamine LTX (Invitrogen), and luciferase activity was measured with a luminometer (VERITAS; Promega). Firefly luciferase activities, derived from each reporter construct, were normalized to Renilla luciferase activities from phRL-SV40.

Stable transfection. To obtain *Fos* expression plasmid (pCAG-Fos-IZ vector), *Fos* cDNA was amplified by RT-PCR from the G1297 cell line with the primer set 5'-ACATGATGTTCTCGGGTTTCAA-3' and 5'-ACTCAGAGGGCCAGCAGCGTGG-3' and subcloned into the *EcoRI* site of the pCAG-EGFP-IZ vector (provided by H. Niwa, RIKEN, Kobe, Japan). pCAG-EGFP-IZ vector or pCAG-Fos-IZ vector was transfected into the G1297 cell line using Lipofectamine LTX Reagent (Invitrogen) and selected for Zeocine resistance (600 µg/ml).

Patients and tumor tissue collection. Anonymized tumor specimens were obtained by surgical resection or biopsy at Gifu University Hospital or Kyoto University Hospital in accordance with an approved protocol from the Institutional Review Board. Total RNA was isolated using a RNeasy mini kit (Qiagen).

ChIP analysis. A total of 5.0×10^6 *EWS/ATF1*-inducible tumor cells was fixed in 1% formaldehyde for 10 minutes, followed by treatment with 1 ml glycine buffer for 5 minutes. Cells were pelleted, washed, and then resuspended in lysis buffer for 30 minutes. After centrifugation, the pellet was resuspended in NP40 buffer with protease inhibitors (Sigma-Aldrich). Sonication was performed using a XL-2000 (MISONIX), after which the supernatant was used as the input sample for immunoprecipitation experiments. Antibodies used were rabbit HA (Cell Signaling) and rabbit normal IgG (Abcam). Protein G-coated magnetic beads were used to purify specific antibody/DNA complexes. After washes, immunoprecipitated DNA was decrosslinked by elu-



tion buffer at 65°C for 12 hours. To remove protein and RNA, samples were incubated with RNaseA for 1 hour at 37°C and proteinase K treatment for 1 hour at 37°C. Samples were purified by PCR purification kit (Qiagen). The amount of DNA immunoprecipitated with HA-tagged protein was quantified by real-time PCR with primers flanking the *Fos* promoter, including the CRE element (forward, 5'-TCCTACACGCGGAAGGTCTAGG-3'; reverse, 5'-TAGAAGCGCTGTGAATGGATGG-3'). Primers 5'-GACTAATTAGTC-GCGGTGGTGG-3' (forward) and 5'-CAGGGTCTTAGTGGGATCAAGG-3' (reverse) were used as a negative control.

Accession number. The profiling data cited in Supplemental Figure 6 are available at GEO (accession no. GSE41123).

Statistics. Statistical analyses were carried out using GraphPad Prism (version 5.01; GraphPad Software). Data were analyzed using ANOVA, and *P* values less than 0.05 were considered statistically significant.

Study approval. Animal experiments were approved by the Gifu University Animal Experiment Committee, and the care of the animals was in accordance with institutional guidelines. All clinical samples were approved for analysis by the Ethics Committee at Kyoto University Graduate School and Faculty of Medicine (Kyoto, Japan). Written informed consent was obtained from all patients with cancers analyzed in this study.

Acknowledgments

The authors thank K. Woltjen and T. Yamamoto (CiRA, Kyoto University) for careful reading of the manuscript and helpful

comments. We also thank T. Motohashi (Tissue and Organ Development Regeneration and Advanced Medical Science) for helpful discussion and the members of the Department of Orthopedic Surgery and Department of Tumor Pathology, Gifu University Graduate School of Medicine; the Department of Orthopaedic Surgery, Graduate School of Medicine, Kyoto University; and the Toguchida and Yamada laboratories for their valuable technical assistance. This study was supported by grants from the Ministry of Education, Culture, Sports, Science, and Technology of Japan and from the Ministry of Health, Labor, and Welfare of Japan.

Received for publication February 28, 2012, and accepted in revised form November 1, 2012.

Address correspondence to: Yasuhiro Yamada, Center for iPS Cell Research and Application (CiRA), Institute for Integrated Cell-Material Sciences (WPI-iCeMS), Kyoto University, 53 Kawahara-cho, Shogoin, Sakyo-ku, Kyoto 606-8507, Japan. Phone: 81.75.366.7034; Fax: 81.75.366.7093; E-mail: y-yamada@cira.kyoto-u.ac.jp. Or to: Takatoshi Ohno, Department of Orthopaedic Surgery, Gifu University Graduate School of Medicine, 1-1 Yanagido, Gifu 501-1194, Japan. Phone: 81.58.230.6333; Fax: 81.58.230.6334; E-mail: takaohno@gifu-u.ac.jp.

1. Enzinger FM. Clear-cell sarcoma of tendons and aponeuroses. An analysis of 21 cases. *Cancer*. 1965; 18:1163-1174.
2. Covinsky M, Gong S, Rajaram V, Perry A, Pfeifer J. EWS-ATF1 fusion transcripts in gastrointestinal tumors previously diagnosed as malignant melanoma. *Hum Pathol*. 2005;36(1):74-81.
3. Deenik W, Mooi WJ, Rutgers EJ, Peterse JL, Hart AA, Kroon BB. Clear cell sarcoma (malignant melanoma) of soft parts: A clinicopathologic study of 30 cases. *Cancer*. 1999;86(6):969-975.
4. Ferrari A, et al. Clear cell sarcoma of tendons and aponeuroses in pediatric patients: a report from the Italian and German Soft Tissue Sarcoma Cooperative Group. *Cancer*. 2002;94(12):3269-3276.
5. Finley JW, Hanypsiak B, McGrath B, Kraybill W, Gibbs JF. Clear cell sarcoma: the Roswell Park experience. *J Surg Oncol*. 2001;77(1):16-20.
6. Eckardt JJ, Pritchard DJ, Soule EH. Clear cell sarcoma. A clinicopathologic study of 27 cases. *Cancer*. 1983;52(8):1482-1488.
7. Kawai A, et al. Clear cell sarcoma of tendons and aponeuroses: a study of 75 patients. *Cancer*. 2007;109(1):109-116.
8. Kindblom LG, Lodding P, Angervall L. Clear-cell sarcoma of tendons and aponeuroses. An immunohistochemical and electron microscopic analysis indicating neural crest origin. *Virchows Arch A Pathol Anat Histopathol*. 1983;401(1):109-128.
9. Segal NH, et al. Classification of clear-cell sarcoma as a subtype of melanoma by genomic profiling. *J Clin Oncol*. 2003;21(9):1775-1781.
10. Bridge JA, Borek DA, Neff JR, Huntrakoon M. Chromosomal abnormalities in clear cell sarcoma. Implications for histogenesis. *Am J Clin Pathol*. 1990; 93(1):26-31.
11. Bridge JA, Steekantiah C, Neff JR, Sandberg AA. Cytogenetic findings in clear cell sarcoma of tendons and aponeuroses. Malignant melanoma of soft parts. *Cancer Genet Cytogenet*. 1991;52(1):101-106.
12. Sandberg AA, Bridge JA. Updates on the cytogenetics and molecular genetics of bone and soft tissue tumors: clear cell sarcoma (malignant melanoma of soft parts). *Cancer Genet Cytogenet*. 2001;130(1):1-7.
13. Kim J, Lee K, Pelletier J. The DNA binding domains of the WT1 tumor suppressor gene product and chimeric EWS/WT1 oncoprotein are functionally distinct. *Oncogene*. 1998;16(8):1021-1030.
14. Lessnick SL, Braun BS, Denny CT, May WA. Multiple domains mediate transformation by the Ewing's sarcoma EWS/FLI-1 fusion gene. *Oncogene*. 1995;10(3):423-431.
15. Pan S, Ming KY, Dunn TA, Li KK, Lee KA. The EWS/ATF1 fusion protein contains a dispersed activation domain that functions directly. *Oncogene*. 1998;16(12):1625-1631.
16. Ohno T, Ouchida M, Lee L, Gatalica Z, Rao VN, Reddy ES. The EWS gene, involved in Ewing family of tumors, malignant melanoma of soft parts and desmoplastic small round cell tumors, codes for an RNA binding protein with novel regulatory domains. *Oncogene*. 1994;9(10):3087-3097.
17. Petermann R, Mossier BM, Aryee DN, Khazak V, Golemis EA, Kovar H. Oncogenic EWS-Flt1 interacts with hSRP7, a subunit of human RNA polymerase II. *Oncogene*. 1998;17(5):603-610.
18. Gonzalez GA, Montminy MR. Cyclic AMP stimulates somatostatin gene transcription by phosphorylation of CREB at serine 133. *Cell*. 1989;59(4):675-680.
19. Comb M, Birnberg NC, Seasholtz A, Herbert E, Goodman HM. A cyclic AMP- and phorbol ester-inducible DNA element. *Nature*. 1986; 323(6086):353-356.
20. Montminy MR, Sevarino KA, Wagner JA, Mandel G, Goodman RH. Identification of a cyclic-AMP-responsive element within the rat somatostatin gene. *Proc Natl Acad Sci U S A*. 1986;83(18):6682-6686.
21. Li KK, Lee KA. MMSP tumor cells expressing the EWS/ATF1 oncogene do not support cAMP-inducible transcription. *Oncogene*. 1998;16(10):1325-1331.
22. Brown AD, Lopez-Terrada D, Denny C, Lee KA. Promoters containing ATF-binding sites are de-regulated in cells that express the EWS/ATF1 oncogene. *Oncogene*. 1995;10(9):1749-1756.
23. Fujimura Y, Ohno T, Siddique H, Lee L, Rao VN, Reddy ES. The EWS-ATF-1 gene involved in malignant melanoma of soft parts with t(12;22) chromosome translocation, encodes a constitutive transcriptional activator. *Oncogene*. 1996;12(1):159-167.
24. Jishage M, Fujino T, Yamazaki Y, Kuroda H, Nakamura T. Identification of target genes for EWS/ATF-1 chimeric transcription factor. *Oncogene*. 2003; 22(1):41-49.
25. Davis IJ, et al. Oncogenic MTF dysregulation in clear cell sarcoma: defining the MIT family of human cancers. *Cancer Cell*. 2006;9(6):473-484.
26. Antonescu CR, Tschernyavsky SJ, Woodruff JM, Jungbluth AA, Brennan MF, Ladanyi M. Molecular diagnosis of clear cell sarcoma: detection of EWS-ATF1 and MTF-M transcripts and histopathological and ultrastructural analysis of 12 cases. *J Mol Diagn*. 2002;4(1):44-52.
27. Granter SR, Weillbaecher KN, Quigley C, Fletcher CD, Fisher DE. Clear cell sarcoma shows immunoreactivity for microphthalmia transcription factor: further evidence for melanocytic differentiation. *Mod Pathol*. 2001;14(1):6-9.
28. Li KK, et al. The melanocyte inducing factor MTF is stably expressed in cell lines from human clear cell sarcoma. *Br J Cancer*. 2003;89(6):1072-1078.
29. Levy C, Khaled M, Fisher DE. MTF: master regulator of melanocyte development and melanoma oncogene. *Trends Mol Med*. 2006;12(9):406-414.
30. Garraway LA, et al. Integrative genomic analyses identify MTF as a lineage survival oncogene amplified in malignant melanoma. *Nature*. 2005; 436(7047):117-122.
31. Speleman F, Delattre O, Peter M, Hauben E, Van Roy N, Van Marck E. Malignant melanoma of the soft parts (clear-cell sarcoma): confirmation of EWS and ATF-1 gene fusion caused by a t(12;22) translocation. *Mod Pathol*. 1997;10(5):496-499.
32. Jiang X, Rowitch DH, Soriano P, McMahon AP, Sucov HM. Fate of the mammalian cardiac neural crest. *Development*. 2000;127(8):1607-1616.
33. Seternes OM, Sorensen R, Johansen B, Loennechen T, Aarbakke J, Moens U. Synergistic increase in c-fos expression by simultaneous activation of the ras/raf/map kinase- and protein kinase A signaling pathways is mediated by the c-fos AP-1 and SRE sites. *Biochim Biophys Acta*. 1998;1395(3):345-360.
34. Ginty DD, Bonni A, Greenberg ME. Nerve growth factor activates a Ras-dependent protein kinase that stimulates c-fos transcription via phosphorylation of CREB. *Cell*. 1994;77(5):713-725.
35. Sassone-Corsi P, Visvader J, Ferland L, Mellon PL, Verma IM. Induction of proto-oncogene fos transcription through the adenylate cyclase pathway:



research article

- characterization of a cAMP-responsive element. *Genes Dev.* 1988;2(12A):1529-1538.
36. Weinstein IB. Cancer. Addiction to oncogenes – the Achilles heel of cancer. *Science.* 2002;297(5578):63-64.
37. Beard C, Hochedlinger K, Plath K, Wutz A, Jaenisch R. Efficient method to generate single-copy transgenic mice by site-specific integration in embryonic stem cells. *Genesis.* 2006;44(1):23-28.
38. Hochedlinger K, Yamada Y, Beard C, Jaenisch R. Ectopic expression of Oct-4 blocks progenitor-cell differentiation and causes dysplasia in epithelial tissues. *Cell.* 2005;121(3):465-477.
39. Haldar M, Hancock JD, Coffin CM, Lessnick SL, Capecchi MR. A conditional mouse model of synovial sarcoma: insights into a myogenic origin. *Cancer Cell.* 2007;11(4):375-388.
40. Riggi N, et al. Development of Ewing's sarcoma from primary bone marrow-derived mesenchymal progenitor cells. *Cancer Res.* 2005;65(24):11459-11468.
41. Adameyko I, et al. Schwann cell precursors from nerve innervation are a cellular origin of melanocytes in skin. *Cell.* 2009;139(2):366-379.
42. Guller M, et al. c-Fos overexpression increases the proliferation of human hepatocytes by stabilizing nuclear Cyclin D1. *World J Gastroenterol.* 2008;14(41):6339-6346.
43. Pandey MK, Liu G, Cooper TK, Mulder KM. Knockdown of c-Fos suppresses the growth of human colon carcinoma cells in athymic mice. *Int J Cancer.* 2012;130(1):213-222.
44. Saez E, et al. c-fos is required for malignant progression of skin tumors. *Cell.* 1995;82(5):721-732.
45. Grigoriadis AE, Schellander K, Wang ZQ, Wagner EF. Osteoblasts are target cells for transformation in c-fos transgenic mice. *J Cell Biol.* 1993;122(3):685-701.
46. Wang ZQ, Grigoriadis AE, Mohle-Steinlein U, Wagner EF. A novel target cell for c-fos-induced oncogenesis: development of chondrogenic tumours in embryonic stem cell chimeras. *EMBO J.* 1991;10(9):2437-2450.
47. Nozawa S, et al. Inhibition of platelet-derived growth factor-induced cell growth signaling by a short interfering RNA for EWS-Flt1 via down-regulation of phospholipase D2 in Ewing sarcoma cells. *J Biol Chem.* 2005;280(30):27544-27551.
48. Yamamoto T, et al. Simultaneous inhibition of mitogen-activated protein kinase and phosphatidylinositol 3-kinase pathways augment the sensitivity to actinomycin D in Ewing sarcoma. *J Cancer Res Clin Oncol.* 2009;135(8):1125-1136.
49. Moritake H, et al. Newly established clear cell sarcoma (malignant melanoma of soft parts) cell line expressing melanoma-associated Melan-A antigen and overexpressing C-MYC oncogene. *Cancer Genet Cytogenet.* 2002;135(1):48-56.
50. Chai Y, et al. Fate of the mammalian cranial neural crest during tooth and mandibular morphogenesis. *Development.* 2000;127(8):1671-1679.
51. Yamauchi Y, et al. A novel transgenic technique that allows specific marking of the neural crest cell lineage in mice. *Dev Biol.* 1999;212(1):191-203.
52. Sakai K, Miyazaki J. A transgenic mouse line that retains Cre recombinase activity in mature oocytes irrespective of the cre transgene transmission. *Biochem Biophys Res Commun.* 1997;237(2):318-324.
53. Srinivas S, et al. Cre reporter strains produced by targeted insertion of EYFP and ECFP into the ROSA26 locus. *BMC Dev Biol.* 2001;1:4.

